Nodal areas in coherent beams

GARRETH J. RUANE[1], GROVER A. SWARTZLANDER, JR.[1,*], SERGEI SLUSSARENKO[2,3], LORENZO MARRUCCI[2], AND MARK R. DENNIS[4]

[1] Chester F. Carlson Center for Imaging Science, Rochester Institute of Technology, 54 Lomb Memorial Drive, Rochester, NY 14623, USA
[2] Dipartimento di Fisica, Università di Napoli Federico II, Complesso Universitario di Monte S. Angelo, Napoli, Italy
[3] Centre for Quantum Dynamics, Griffith University, Brisbane, Queensland 4111, Australia
[4] H. H. Wills Physics Laboratory, University of Bristol, Bristol BS8 1TL, United Kingdom
[*] Corresponding author: grover.swartzlander@gmail.com

Compiled December 23, 2014

Whereas nodal points having zero amplitude are well-known wave phenomena, destructive interference across a continuous area is exceedingly rare. In fact these strange states seem to defy nature's "abhorrence of nothingness." Philosophizing aside, we report general schemes for constructing a nodal area (or black hole) in a spatially coherent beam of light by use of a lossless phase mask. Theoretical, numerical, and experimental results are presented. Nodal areas are important for high contrast imaging, laser surfacing, radiation shielding, and other structured light applications. Moreover, these results transcend optics and open the possibility of achieving nodal area wave functions in quantum, acoustic, and other coherent wave systems.

OCIS codes: *(050.4865) Optical vortices; (100.5090) Phase-only filters; (160.3710) Liquid crystals; (070.0070) Fourier optics and signal processing; (350.1260) Astronomical optics.*

http://dx.doi.org/10.1364/optica.XX.XXXXXX

Perhaps no other phenomenon distinguishes waves from particles better than total destructive interference. Interference provides the basis for an exhausting list of technologically important devices in both classical and quantum wave systems. Any new approach which provides a different means to achieve interference is therefore of great general interest. For example, the advent of optical vortices [1–4] has lead to applications in areas as diverse as astronomical and sub-resolution imaging [5–7], spinning Bose-Einstein condensates [8], and quantum entanglement [9]. A vortex wave function is distinguished by a nodal point in the beam cross section, around which the scalar phase varies azimuthally by a non-zero integer multiple of 2π. Zero-valued states in a system and their asymptotic limit are intriguing manifestations of nature [10] and attract considerable experimental and theoretical attention. Vortex and other harmonic wave functions were significant in the advancement of quantum mechanics and superfluid states [11–13]. Extensions of these topics spawned interest in fluid-like phenomena in lasers [2], nonlinear refractive media [4], and orbital optical momentum [14]. The remarkable discovery of the formation of a nodal *area* by use of a vortex [5, 6, 15] or four-quadrant [16] phase mask could similarly excite widespread interest. In those cases a circular nodal area was generated when the initial beam was defined by a uniformly illuminated circular aperture.

The motivation of this report is to explore whether other types of apertures and phase masks afford the formation of nodal areas. In fact, we make the conjecture that any apertured beam of finite support may be optically transformed with a lossless phase element such that support of the final beam is complementary to the original. Loosely phrased, we assert that a beam can be "turned inside out" without loss of power by use of a phase mask in the focal plane, producing a black hole in the transverse cross-section of the beam. (Diffraction of this hole is shown in Supplement 1.)

An analytical transformation that turns an apertured beam inside out was first realized for a circular aperture and was the basis of a high contrast coronagraph [5, 6, 16]. An elliptically apertured beam was later proposed to produce an elliptical nodal area [17]; experimental verification is reported here by use of a so-called q-plate [18, 19]. Two confirmed experimental examples however do not constitute a proof of the conjecture. As further evidence we provide an analytical solution for a wide variety of azimuthally invariant apertures that can be turned into nodal areas by use of a vortex phase mask. Additionally, we provide numerical examples using a point-by-point iterative phase-retrieval algorithm [20, 21] to design phase elements for an aperture of arbitrary shape. Developing a proof of the conjecture for any aperture function is, as for related phase retrieval problems, complicated by the underdetermined nature of the problem.

The discovery of other closed structures admitting nodal areas may be useful in optics for high contrast imaging applications, optical patterning, or light-matter interactions. We point out that the zero-amplitude state is an idealized concept that in practice can only be approached asymptotically owing to limi-

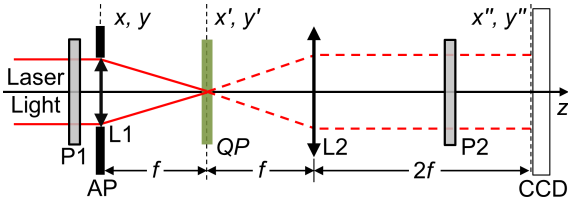

Fig. 1. Optical configuration for producing a nodal area with a q-plate (QP). Uniform laser light that is circularly polarized by polarizing optics P1 enters an aperture AP at the x, y plane. Lens L1 focuses the transmitted light onto QP. Lens L2 forms the exit pupil at the x'', y'' plane. The second set of polarizing optics P2 is circularly cross-polarized to P1. The nodal area appears at the x'', y'' plane, where an image is captured by a CCD.

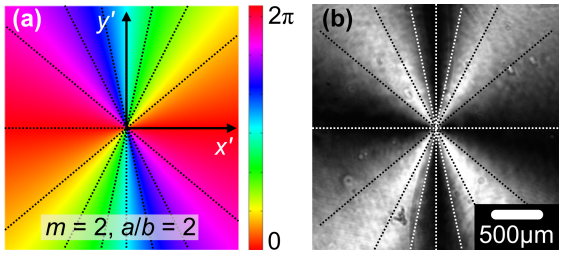

Fig. 2. Transmission of an elliptical q-plate. (a) Phase of the elliptical vortex function $\Phi(x', y')$ with $m = 2$ and $a/b = 2$. Lines of constant phase (dotted) are indicated in steps of $\pi/4$. (b) Zoomed-in image of the fabricated, 1 cm×1 cm, elliptical q-plate placed between orthogonal linear polarizers, showing the expected irradiance pattern: $\sin^2(2\alpha)$.

tations such as wave front aberrations, non-paraxial waves, the degree of coherence [22], and quantum mechanics [23].

Let us first review how a circular nodal area ("ring of fire" or corona) is produced by use of a vortex phase mask [5, 6, 15]. A circular aperture of radius a transforms into an isomorphic circular nodal area in a 4-f optical system, illustrated in Fig. 1, by centering the vortex mask with the Airy disk in the focal plane formed with lens L1. Transmission of the optical field through the vortex element is represented by the function $t_m(x', y') = \exp(im\theta')$, where m is a nonzero even integer called the topological charge, and θ' is the azimuth in the transverse x', y' plane (i.e. $\tan\theta' = y'/x'$). Various methods may be used to produce the phase mask, including photoalignment of nematic liquid crystals [18, 19]. The transformed aperture function in the x'', y'' plane may be understood as a convolution of the circular aperture with the Fourier transform (FT) of the vortex mask transmission function [24] $FT\{t_m(x', y')\} = \gamma_m (1/r'')^2 \exp(im\theta'')$, where r'' and θ'' are polar coordinates in the x'', y'' plane, $\gamma_m = (-i)^m mf/k$, f is the focal length of the lenses, $k = 2\pi/\lambda$, and λ is the wavelength. Rather than re-imaging the aperture, this system remarkably diffracts all the light outside the aperture, resulting in a black nodal area where the field is zero-valued in the interior region ($r'' < a$). In the case where $m = 2$, the exterior field is given by $E(x'', y'') = (a/r'')^2 \exp(i2\theta'')$ (see Supplement 1 for derivation).

For any linear superposition of vortex transmission functions having nonzero even values of topological charge, a circular nodal area is expected to form [24]. Such a superposition, however, does not change the circular size or shape of the nodal area. Therefore, there is not a unique means of transforming a circular aperture into a nodal area. This suggests that for other aperture types, there may also be families of modes that represent nodal areas.

As an important example, consider a uniformly illuminated elliptical aperture. The modes that produce a nodal area can be found by mapping the circular modes onto the ellipse [17]. A focal plane phase element that accomplishes this is described by a skewed vortex mask transmission function: $\tilde{t}_m(x', y') = \exp(im\Phi)$, where $\Phi = \arctan(by'/ax')$, where m is a non-zero even integer, and a and b are respectively the major and minor axis of the aperture.

Experimental Verification: The required phase Φ was produced by means of a q-plate; i.e., a spatially variant half-wave retarder with the fast axis orientation described by $\alpha(x', y') = q\arctan(by'/ax') + \alpha_0$, where $q = |m/2|$ and α_0 are constants (see Supplement 1 for fabrication details) [18, 19]. The transmitted circularly polarized components of the field may be expressed $E_{R,L} = e^{\pm i2\alpha} E_{L,R}$, where E_R and E_L are respectively the right and left hand circular polarization components of the incident field. Interestingly, the two output components each have a vortex phase and a polarization orthogonal to the input state [25]. For $m = 2$, the fields in the exit pupil plane may be written $U_{R,L}(x'', y'') = E_{L,R}(1/\rho'')^2 \exp(\pm i2\Theta)$, where $\rho'' > 1$, $\Theta = \arctan(ay''/bx'')$, and $\rho'' = [(x''/a)^2 + (y''/b)^2]^{1/2}$. Both polarization components are zero-valued if $\rho'' < 1$.

For our experiment (see Fig. 1), an expanded collimated He-Ne laser beam ($\lambda = 632.8$ nm) was made circularly polarized by use of a linear polarizing filter followed by a quarter wave retarder (P1). The central nearly uniform region of the beam was then transmitted through an elliptical aperture (AP) with major and minor axes $a = 1.50$ mm and $b = 0.75$ mm (see Fig. 3(a)). The elliptical beam was focused by lens L1 onto the voltage-controlled q-plate, with which we achieved half-wave phase-retardation condition with a 6.6 V, 6 kHz sinusoidal signal [19]. The diameter of the focal spot was 515 μm along the x' axis and 1030 μm along the y' axis. We note that the focal spot is at least 20 times larger than the 25 μm central deformation of the q-plate. Lenses L1 and L2 both have a focal length of 1 m, and diameters 25.4 mm and 50.8 mm, respectively. The field lens L2 imaged the entrance pupil on a CCD array in the x'', y'' plane. An image of the entrance pupil forms on the detector array when the q-plate is removed from the system, or when the center of the q-plate is displaced from the center of the beam, as shown in Fig. 3(a). However, when these centers coincide, an elliptical nodal area appears as seen in Fig. 3(b). A circular polarizer analyzer (P2) was used to remove light that may have been transmitted in the wrong polarization state, owing to irregularities in the q-plate. A quantitative measure of the nodal area contrast is the fraction of the total beam power across the innermost half of the nodal region. We achieved an experimental value of

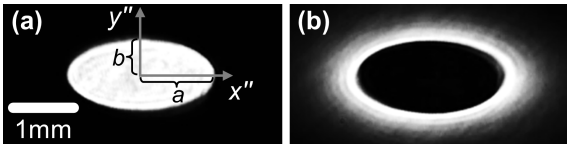

Fig. 3. Experimental verification of an elliptical nodal area. Image of the elliptical aperture without (a) and with (b) the elliptical vortex q-plate.

0.24% – a remarkable result given that this is the first reported measurement of an elliptical nodal area (see Supplement 1 for details).

Let us explore whether other aperture types can produce a nodal area by means of a lossless phase mask. Realizing that circular symmetry provides a path for generating circular nodal areas, we considered the important case of an annular aperture, as found in many telescopes and reflecting microscopes. The discovery of nodal areas for this system could provide a path toward extreme high-contrast astronomical imaging. For reasons that will become obvious below, we replace the "hard" central obscuration with a soft obscuration so that for $r/a < 1$ (i.e., inside the outer radius) $A(r) = 1 - \exp\left[-(r/w)^2\right]$, where w is a width parameter [see Fig. 4(a)]. For $r/a > 1$, $A(r) = 0$. The use of pupil apodization may provide practical advantages to an imaging system [26–29]. We propose that, in general, a nodal area can be found if we replace the circularly symmetric aperture function with a truncated linear superposition of zero-order radial Zernike polynomials, $R_n^0(r/a)$:

$$\tilde{A}(r) = \sum_{n=0}^{N} c_n R_n^0(s), \tag{1}$$

where $c_n = 2(n+1)a^2 \int_0^1 A(s) R_n^0(s) ds$ and $s = r/a$. Zernike polynomials are the only presently known basis functions that transform into nodal areas. The value of N may be selected based on engineering and performance metrics, such as the ease of mask fabrication and the desired darkness of the nodal area. For the Gaussian central obscuration function above, $A(r)$, we find c_n^2 rapidly decreases as $\exp(-n^2)$. It is easily shown by direct integration that a nodal area is formed in the exit pupil plane if a vortex phase mask having an even valued topological charge $|m| > N+1$ is inserted into the focal plane of the telescope. A vortex phase mask having $|m| = 6$ could then provide a perfectly black nodal area for an engineered aperture $\tilde{A}(r)$, where $N = 4$. What is more, this result suggests that the non-truncated soft aperture function, $A(r)$ would produce a dark, but non-ideal nodal area, as long as the value of $|m|$ is sufficiently large. In this case the quality of the nodal area may be quantitatively expressed as the ratio of the beam power within the nodal area and the total power transmitted through the aperture, $\eta = P_{in}/P_{tot}$, where $P_{in} = a^{-2} \sum_{n=m}^{\infty} c_n^2/(n+1)$. For the soft aperture function $A(r)$ shown in Fig. 4(a) (with $w/a = 0.56$), we find that an $m = 6$ vortex phase element (see Fig. 4(b)) provides a power ratio of $\eta = 10^{-6}$. The numerically determined exit pupil amplitude shown in Fig. 4(c) exhibits a nearly ideal nodal area, as expected. Considering practical limitations such as aberrations and non-ideal aperture functions, it may be difficult and unnecessary to achieve smaller values of η. Abhorring the zero state, nature only allows us to asymptotically approach the ideal value, $\eta = 0$.

Numerical Solutions: Now that we have established additional means of achieving nodal areas (e.g., circle remappings and Zernike decompositions), we wish to explore the possibility that any aperture function can be generally transformed. To our knowledge it is currently unknown whether the desired lossless transmission functions mathematically exist. In fact, it is difficult to imagine how other apertures and phase masks could also produce a nodal area based on either a convolution or direct integral point of view. Nevertheless, the question may be formulated as a phase retrieval problem. Consider a 4-f imaging system with an aperture function $A(x,y)$ and focal plane mask having a transmission function $t(x',y') = \exp[i\Phi(x',y')]$. The field at the focal plane just before the phase element is given by the FT of the aperture function $F(x',y') = FT\{A(x,y)\}$. Similarly, the exit pupil field is the inverse FT of the focal plane field $G(x'',y'') = FT^{-1}\{F(x',y')\exp[i\Phi(x',y')]\}$. We wish to calculate the phase function $\Phi(x',y')$ necessary so that $G(x'',y'') = 0$ over the support of $FT^{-1}\{F(x',y')\}$. For convenience, let us again consider a real rotationally symmetric aperture. Owing to symmetry we allow for the possibility of both azimuthal and radial variations of the phase mask: $\Phi = m\theta' + \mu(r')$, where $\mu(r')$ is a real valued function. (Note that above, we only assumed azimuthal variations of the phase mask.) The exit pupil field may be expressed in terms of an mth order Hankel transform $G(r'',\theta'') = H_m\{F(r')e^{i\mu(r')}\}e^{im\theta''}$. The solution for the Hankel transform may be written as the product of amplitude and phase functions: $H_m\{F(r')e^{i\mu(r')}\} = g_0(r'')e^{i\nu(r'')}$. Being unsuccessful at finding analytical expressions for $\mu(r')$, $g_0(r'')$, and $\nu(r'')$, we instead applied a numerical phase retrieval approach, namely a modified Gerchberg-Saxton (G-S) algorithm [20, 21]. Although this approach iteratively finds a non-unique solution for the phase mask that produces a nodal area, the solutions may be complicated and impractical from a fabrication point of view. The selection of a simple initial guess for the function $\mu(r')$ may, however, lessen the complexity of the final iterative solution.

The iteration scheme proceeds as follows. The field at the exit pupil plane where we hope to find a nodal area is the FT of the product of the mask transmission function and the point spread function (FT) of the aperture. At each iterative step, if the nodal region is not zero-valued, it is forced to zero, and then the FT of the field at the exit pupil is computed. This produces new focal plane amplitude and phase functions. We replace this new amplitude function with actual PSF of the system, and then a new exit pupil field is computed. This process is iterated until the power in the nodal area approaches zero. At that point the final phase mask profile is computed.

As an example, Fig. 4(d-f) shows an annular aperture having a hard central obscuration, along with the computed phase mask and nodal area. The ratio of inner and outer radii was 0.38. In this case we used a vortex phase with $m = 2$, and as a first guess in the iteration, we assumed an axicon phase, $\mu(r') = \pm\alpha r'$, where $\alpha > 2ka/f$. As designed, the nodal area in Fig. 4(f) has the same diameter as the outer diameter of the

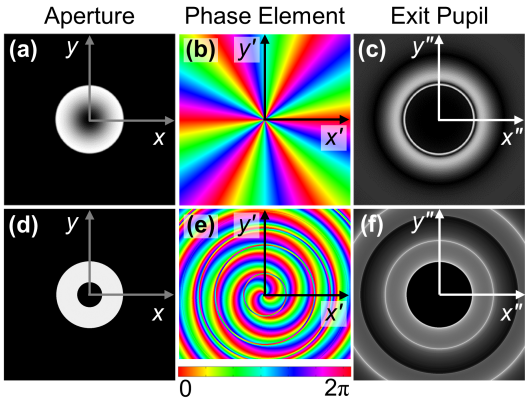

Fig. 4. (a) An apodized annular aperture matched with (b) an $m = 6$ vortex phase element generates (c) a dark region with radius equal to the outer radius of the aperture. (d)-(f) Same as (a)-(c), but with (d) an annular aperture, (e) the numerically computed element, and (f) the corresponding nodal area.

annulus. The construction of such a phase mask depicted in Fig. 4(e) may be possible with advanced fabrication techniques [25]. Undoubtedly, the computed structures are indicative of modal symmetries and relationships yet to be analytically discovered. Comparing the G-S outcome with the Zernike approach above, we find for an annular aperture having a hard central obscuration, the Zernike method would requires a vortex mask of high topological charge, whereas the G-S algorithm allows for a low vortex charge ($m = 2$), accompanied by radial structure in the phase mask.

This, and other G-S examples not reported here, tends to confirm our conjecture that a phase-only (lossless) mask can be found to produce a nodal area having the shape of an arbitrary entrance pupil (see Supplement 1 for an additional solution). Undoubtedly, the computed structures are indicative of modal symmetries and relationships yet to be analytically discovered. Such relationships are likely related to sets of orthogonal functions is some basis that depends on the symmetries of the aperture function.

Conclusions: Nodal areas are an intriguing manifestation of destructive interference across an extended region in a given cross-section of a beam of light. Previously, only circular nodal areas have been observed. Here we have described the first experimental observation of an elliptical nodal area, produced by use of a uniformly illuminated elliptical aperture and a specially designed "elliptical vortex q-plate". After questioning whether it is possible to create nodal areas from more complicated aperture functions and phase plates, we provided both analytical and numerical approaches – each supporting (but not proving) the conjecture that nodal areas can indeed be formed. By use of Zernike mode decomposition, we have presented a method to create a nodal area from any azimuthally invariant circular aperture, such as a softly obscured annular aperture. In that case a vortex phase mask of high topological charge is typically required. This method is also suitable for elliptical apertures by mapping to a circular coordinate system. Finally, we illustrated how a Gerchberg-Saxton phase retrieval algorithm [20, 21] may be used to design a focal plane phase mask that produces a nodal area. The latter result hints of yet undiscovered symmetries which suggest to us the possibility of elegant solutions supporting nodal areas for any aperture function. We believe there is no single unique phase mask that transforms a given aperture into a nodal area. It is likely that the G-S numerical approach provides a linear combination of the underlying basis set of solutions. In optics, beams containing nodal areas may find increasing importance in applications involving structured light, such as radiation shielding, laser surfacing, radiation pressure, high contrast imaging, and dense channel line-of-sight telecommunication. We anticipate that additional experimental and theoretical investigations will help uncover general mathematical properties of nodal areas, as well as identify new applications of structured darkness in optics and other wave systems.

FUNDING INFORMATION

U.S. Army Research Office (W911NF1110333-60577PH); National Science Foundation (ECCS-1309517); FET-Open Program within the 7th Framework Programme of the European Commission, Phorbitech (255914).

ACKNOWLEDGMENTS

From RIT we thank Thomas Grimsley, Lindsay Quandt, and Michael Rinkus, for assistance with mask fabrication and photographic work.

REFERENCES

1. J. F. Nye and M. V. Berry, Proc. R. Soc. A. **336**, 165 (1974).
2. P. Coullet, L. Gil, and F. Rocca, Opt. Commun. **73**, 403 (1989).
3. V. Y. Bazhenov, M. V. Vasnetsov, and M. S. Soskin, Pis'ma Zh. Eksp. Teor. Fiz. **52**, 1037 (1990) [JETP Lett. **52**, 429 (1990)].
4. G. A. Swartzlander, Jr. and C.T. Law, Phys. Rev. Lett. **69**, 2503 (1992).
5. D. Mawet, P. Riaud, O. Absil, and J. Surdej, Astrophys. J. **633**, 1191 (2005).
6. G. Foo, D. M. Palacios, and G. A. Swartzlander, Jr., Opt. Lett. **30**, 3308 (2005).
7. V. Westphal and S. W. Hell, Phys. Rev. Lett. **94**, 143903 (2005).
8. K. C. Wright, L. S. Leslie, and N. P. Bigelow, Phys. Rev. A **77**, 041601 (2008).
9. A. Mair, A. Vaziri, G. Weihs, and A. Zeilinger, Nature **412**, 313 (2001).
10. M. V. Berry, Phys. Today **55**, 10 (2002).
11. L. Landau, Phys. Rev. **60**, 356 (1941).
12. V. L. Ginzburg and L. P. Pitaevskii, Zh. Eks. Teor. Fiz. **34**, 1240 (1958), [Sov. Phys. JETP **7**, 858 (1958)].
13. L. P. Pitaevskii, Zh. Eks. Teor. Fiz. **40**, 646 (1961), [Sov. Phys. JETP **13**, 451 (1961)].
14. L. Allen, S. M. Barnett, and M. J. Padgett, *Optical Angular Momentum* (Institute of Physics Publishing, Bristol, 2003).
15. S. N. Khonina, V. V. Kotlyar, M. V. Shinkaryev, V. A. Soifer, and G. V. Uspleniev, J. Mod. Opt. **39**, 1147 (1992).
16. D. Rouan, P. Riaud, A. Boccaletti, Y. Clénet, and A. Labeyrie, Publ. Astron. Soc. Pac. **112**, 1479 (2000).
17. G. J. Ruane and G. A. Swartzlander, Jr., Appl. Opt. **52**, 171 (2013).
18. L. Marrucci, C. Manzo, and D. Paparo, Phys. Rev. Lett. **96**, 163905 (2006).
19. S. Slussarenko, A. Murauski, T. Du, V. Chigrinov, L. Marrucci, and E. Santamato, Opt. Express **19**,4085 (2011).
20. R. W. Gerchberg and W. O. Saxton, Optik **35**, 237 (1972).
21. J. R. Fienup, Appl. Opt. **21**, 2758 (1982).
22. G. A. Swartzlander, Jr. and R. I. Hernandez-Aranda, Phys. Rev. Lett. **99**, 163901 (2007).
23. M. V. Berry and M. R. Dennis, J. Opt. A: Pure Appl. Opt. **6**, S178 (2004).
24. G. A. Swartzlander, Jr., J. Opt. A: Pure Appl. Opt. **11**, 094022 (2009).
25. Z. Bomzon, G. Biener, V. Kleiner, and E. Hasman, Opt. Lett. **27**, 1141 (2002).
26. O. Guyon, Astron. Astrophys. **404**, 379 (2003).
27. R. Soummer, Astrophys. J. **618**, L161 (2005).
28. A. Carlotti, R. Vanderbei, and N. J. Kasdin, Opt. Express **19**, 26796 (2011).
29. D. Mawet, L. Pueyo, A. Carlotti, B. Mennesson, E. Serabyn, and J. K. Wallace, Astrophys. J. Suppl. Ser. **209**, 7 (2013).